International Journal of Thermophysics, Vol. 23, No. 1, January 2002 (© 2002)

Dynamic Behavior of a Pure Fluid at and Near Its Critical Density Under Microgravity and 1*g*[1]

C. Bartscher[2] and J. Straub[2, 3]

A new sample cell allowing accurately measurable density quenches was developed for further and systematic investigation of dynamic temperature propagation, or the piston effect. Several experiments were performed under 1*g* and microgravity during and in preparation for the Perseus mission in 1999. The starting temperatures ranged in the one-phase state between 1 and 1000 mK above T_c, while the density varied between $0.7\rho_c < \rho < 1.3\rho_c$. The method for the determination of the isentropic difference coefficients $(\Delta\rho/\Delta T)_S$, $(\Delta\rho/\Delta p)_S$, and $(\Delta T/\Delta p)_S$ is explained. The coefficients are in reasonable agreement with the equation of state for SF_6, and the difference between the ground and the microgravity experiments is discussed. The advantage of the density quench method in contrast to the temperature quench method is demonstrated, particularly with regard to the influence of convection.

KEY WORDS: Alice 2 Facility; dynamic temperature propagation; isentropic coefficients; microgravity; Perseus mission; piston effect; SF_6.

1. INTRODUCTION

A near-critical fluid is highly compressible. Therefore, a sudden rise in temperature in the wall of a sample cell of a finite volume, which causes a thermal expansion of the fluid in the boundary layer, results in a compression of the bulk fluid, with an average pressure and temperature increase [1–3] in the bulk. This effect is known as the "piston effect" (PE), or dynamic temperature propagation. Assuming that the temperature gradients outside the boundary layer are negligible and that no energy is

[1] Paper presented at the Fourteenth Symposium on Thermophysical Properties, June 25–30, 2000, Boulder, Colorado, U.S.A.

[2] Technische Universität München, Lehrstuhl für Thermodynamik, Boltzmannstrasse 15, D-85748 Garching, Germany.

[3] To whom correspondence should be addressed. E-mail: bartscher@td.mw.tum.de

0195-928X/02/0100-0077/0 © 2002 Plenum Publishing Corporation

dissipated, the compression is adiabatic and isentropic. The energy transport is a mechanical process, propagating like a pressure wave to the center of the cell, and is defined by the speed of sound w_s and the isentropic compressibility χ_s [4]. This means that for compressible fluids the thermal propagating process is not caused exclusively by thermal diffusivity, something that had been assumed for a long time and that is true for incompressible fluids. Neglecting the fact that a critical fluid is compressible, such diffusion would then result in long thermal relaxation processes as the thermal diffusion approaches zero near the critical point.

Recent piston effect experiments were performed using either a surface heater [1] or a thermistor as a point heater [5]; however, a large power input for several seconds was necessary before measurable results could be achieved in the fluid due to the small heater surface. Since many analytical approaches favor a step-like temperature change, we used a different method by performing rapid ($t < 0.4$ s) density quenches of the whole fluid while the wall temperature remained constant as the boundary condition.

By measuring temperature and pressure changes in the fluid (ΔT, Δp) fast enough and at a sufficiently high resolution, the difference coefficients can be approximately regarded as differential coefficients, when the step size of $\Delta\rho$ is small. With this condition several isentropic coefficients $(\frac{\partial p}{\partial \rho})_s$, $(\frac{\partial T}{\partial \rho})_s$, and $(\frac{\partial p}{\partial T})_s$ can be calculated. From the temperature and average density change, the isentropic expansion coefficient α_s can be determined using

$$\alpha_s = -\frac{1}{\rho}\left(\frac{\partial \rho}{\partial T}\right)_s, \qquad \text{with} \quad \left(\frac{\partial \rho}{\partial T}\right)_s \sim \left.\frac{\Delta \rho}{\Delta T}\right|_s \tag{1}$$

The isentropic compressibility χ_s can be determined from the related average change in pressure Δp,

$$\chi_s = \frac{1}{\rho}\left(\frac{\partial \rho}{\partial p}\right)_s, \qquad \text{with} \quad \left(\frac{\partial \rho}{\partial p}\right)_s \sim \left.\frac{\Delta \rho}{\Delta p}\right|_s \tag{2}$$

and with Δp and ΔT, the isentropic tension coefficient β_s,

$$\beta_s = \frac{1}{p}\left(\frac{\partial p}{\partial T}\right)_s, \qquad \text{with} \quad \left(\frac{\partial p}{\partial T}\right)_s \sim \left.\frac{\Delta p}{\Delta T}\right|_s \tag{3}$$

Using these isentropic coefficients, further thermodynamic relations can be derived, such as the speed of sound and the isochoric specific heat capacity,

$$w_s = \rho \chi_s^{-\frac{1}{2}} \qquad \text{and} \qquad c_v = -\frac{\rho}{PT}\alpha_s \beta_v, \qquad \text{with} \quad \beta_v = \frac{1}{p}\left(\frac{\partial p}{\partial T}\right)_V \tag{4}$$

These can be used to check the consistency of thermodynamic equations, especially in the near-critical region, where several thermodynamic properties diverge.

2. EXPERIMENTAL SETUP

To perform accurate density quenches and measure the corresponding dynamic pressure and temperature response, we developed a sample cell (Fig. 1) that was divided into a compensation and an observable measurement volume. The measurement volume had a diameter and height

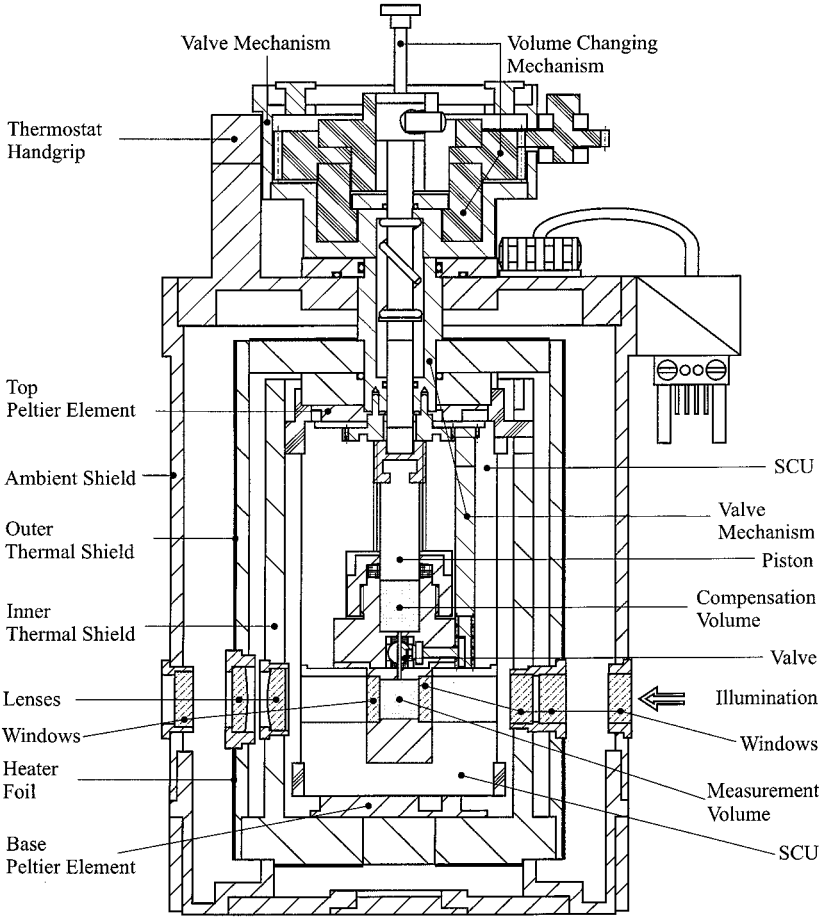

Fig. 1. Aluminum fluid cell and sample cell unit (SCU) integrated in the three-shell thermostat unit (THU).

both equal to 12 mm, with sapphire windows at both ends, giving the cell a cylindrical shape. The two volumes were interconnected through a canal with a diameter of 1 mm which passed through a ball valve.

The valve was necessary for two reasons. Only the measurement volume could be observed by video, and to prevent it from being influenced by unseen effects occurring inside the compensation volume, both volumes had to be separated from each other. By closing the valve after each density setting, the shape and the volume-to-surface ratio of the measurement volume remained unchanged, leaving the density as the only variable. This simplified the comparison of the phase separation experiments and the piston PE experiments.

In the 12-mm-diameter compensation volume, a piston could be moved back and forth in small and rapid steps over a magnitude of $\Delta\rho = 1.0\%\ \rho_c$. The maximum possible piston translation of 15 mm allowed initial average density $\bar{\rho}$ settings in the range of $0.7\rho_c < \bar{\rho} < 1.35\rho_c$. In the measurement volume an "ENTRAN" piezoelectric-resistive pressure sensor was installed, as well as three very small thermistors, each bead 0.25 mm in diameter and with a thermal time constant of 10 ms. One thermistor (T_1) was installed within 0.5 mm of the center of the cell, and the second (T_2) 0.67 mm off the aluminum wall inside the fluid. A third thermistor (T_3) was installed in the wall within 1 mm of the fluid to quantify the effect of the changing fluid temperature on the wall of the cell after the density quenches.

The piston, the valve, their mechanisms, and the fluid cell were inserted into an aluminum cylinder (60 mm in diameter, 115 mm in height), known as the sample cell unit (SCU). Three additional thermistors distributed over the SCU functioned as measurement, control, and overheat sensors for the facility's temperature control. The SCU was mounted in a three-shield thermostat built by the van der Waals–Zeeman Laboratory at the University of Amsterdam (Fig. 1). For microgravity (μg) measurements on MIR, the thermostat was inserted into the Aerospatiale-built and CNES-funded Alice 2 facility which provided a very stable temperature environment (40 $\mu K \cdot h^{-1}$), with a relative resolution of 100 μK [6]. Since on-line data analysis during the μg mission was not possible, the temperature and pressure data were collected at a rate of 25 Hz during PE measurements and stored on PCMCIA cards, while the video images of the fluid cell were recorded on DAT tape. The data had to be returned to Earth by the cosmonauts for post-experiment analysis.

Unfortunately, the implementation of a stepping motor for the piston movements was not possible, as the experiments were proposed after Alice 2 had been built and transported to MIR. No interface was available for the necessary power supply and coordinated control possibilities, therefore,

all mechanical movements were performed by hand by the cosmonaut, with a special tool. This naturally led to a wider spectrum in terms of quench time, varying mostly in the small range of $0.28\ \text{s} < t < 0.44\ \text{s}$.

For the 1g reference experiments an engineering model of the Alice 2 facility and a laboratory setup were used, with a temperature control identical to the Alice 2 facility and therefore exhibiting similar control stability. The main difference in the laboratory setup lay in the data acquisition using a Keithley 2001 multiscanner. It allowed only a 10-Hz measurement frequency per sensor; however, with an adequate filter and a resolution of 2 mbar of the pressure sensor data, the noise level of 3.8 mbar rms was about 10 times better than that of the facility. The temperature resolution of 0.6 mK with a noise level of 0.4 mK rms was similar for both the facility and the setup.

3. EXPERIMENT EXECUTION

To minimize thermal leaks, the piston mechanism was usually disconnected from the SCU, particularly during phase separation experiments. However, for the adjustment of the average fluid's density before each experiment run and the described PE experiments, the piston mechanism had to be fully inserted. For initialization of the fluid density, the cell was homogenized at temperatures far above the critical temperature in the one-phase region, typically $T_c + 2$ K. Then the valve was opened and the fluid was gradually cooled to a starting temperature value in the range of $1\ \text{mK} < T - T_c < +1000\ \text{mK}$. Before the PE experiment was performed, sufficient time was provided to reach a temperature equilibrium and homogeneous density distribution in the fluid. The subsequent density quench, expansion or compression, had to occur in a rapid and uniform manner, while the video images were recorded by the Alice 2 facility synchronized with the temperature and pressure data acquisition at a 25-Hz rate.

A series of PE experiments was performed under 1g and μg with SF_6 as the test fluid ($T_c = 318.717$ K, $p_c = 3.7545$ MPa, $\rho_c = 742\ \text{kg}\cdot\text{m}^{-3}$ [7]). The starting temperatures before the quench were typically at $T - T_C = 10$, 50, 100, 200, 500, and 1000 mK for 1g and $T - T_C = 30$, 50, and 100 mK for μg, with an average starting density range from 0.7 to $1.35\rho_c$. The typical quench time lasted about 350 ± 100 ms and the quench size was of a magnitude of $\Delta\rho_{\text{quench}} = 0.0088\rho_c \pm 5\%$.

4. EXPERIMENTAL RESULTS

For the calculation of the isentropic coefficients from the measurement data, some deficiencies due to the nature of the experiment had to be taken

into account. Since the frequency of data acquisition was either 25 or 10 Hz (depending on which facility was used) and we tried to keep the quench time as short as possible (typically around 350 ms), only very few data points could be acquired during the quench sequence. Hence, it was very unlikely that, within the time gap of either 40 or 100 ms between each single data point, the highest temperature point acquired was the actual largest value (e.g., data point 3 in Fig. 2) that should have been reached due to the quench. Looking at the run of the curve in Fig. 2, the maximum had to be between the marked data points 2 and 3, and the beginning of the quench between data points 0 and 1. Therefore, mathematical fits and extrapolations had to be made through the data points of the interval before the quench, the interval during the quench, and the relaxation phase after the end of the quench. This led to the starting point of the quench, marked "a," and the new temperature maximum, marked "b," and its respective point of time.

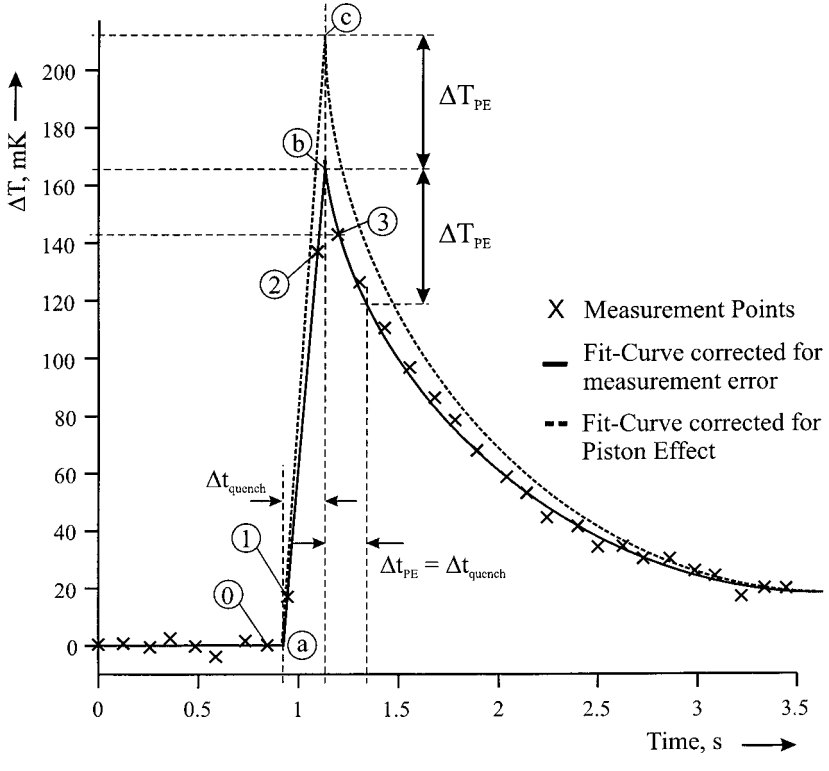

Fig. 2. Two-step method to correct data for measurement deficiency and PE influence due to length of quench.

The influence of the PE on the development of the temperature change also had to be taken into consideration. Although the quenches were performed quickly, the PE is initiated as soon as the temperatures of the fluid and the wall start to differ. In addition, convection sets in on ground, counteracting the temperature rise with the PE as soon as the quench is started. Both effects prevent the fluid from reaching its theoretical temperature peak. To consider those effects in the calculation of the coefficients, we first calculated the temperature drop (ΔT_{PE}) from the maximum temperature (point b in Fig. 2) during a time frame Δt_{PE}, which was equal to the length Δt_{quench} of the quench. Then this temperature difference was added to the previously calculated temperature maximum, resulting in a new theoretical maximum (point c), which is corrected for measurement and piston effect errors (solid line in Fig. 2).

Another important fact was that with this experiment setup it was not possible to actually measure the temporal change of the density ($\partial\rho/\partial t$) during the quench. Instead, the total density difference $\Delta\rho$ had to be used, which could be determined within a 5 to 8% uncertainty. As mentioned in Section 1, the isentropic coefficients were also calculated from pressure and temperature differences (Δp and ΔT), and not from differential changes. This simplification was legitimate as long as the quench time (Δt) was kept short, which, in turn, did not allow the differential calculation of pressure or temperature changes, due to the small number of acquired data points during the quench.

Under the assumption that the compression is adiabatic and isentropic, we then calculated the isentropic coefficients under the consideration of the aforementioned corrections. The importance of the shortness of the quench to our assumptions can be seen in Table I.

With the shortest quench time, $\Delta t_1 = 0.207$ s, the calculated isentropic coefficient $(\Delta\rho/\Delta T)_S$ deviates from the theoretical value by only 8.3% and is, therefore, within the accuracy of $\Delta\rho$, whereas in the case of the 2.5× longer quench ($\Delta t_3 = 0.533$ s), the calculated value already deviates by 27.6%. Because the accuracy of determining the density difference remains the same for all three examples, this shows that with longer quench times it becomes more and more difficult to compensate for the influence of the PE

Table I. Influence of the Quench Time Δt on the Result Accuracy

	$\Delta t_1 = 0.207$ s	$\Delta t_2 = 0.267$ s	$\Delta t_3 = 0.533$ s
$(\partial\rho/\partial T)_{theory}$	25.79 kg·m^{-3}·K^{-1}	25.79 kg·m^{-3}·K^{-1}	25.79 kg·m^{-3}·K^{-1}
$(\Delta\rho/\Delta T)_{calculation}$	27.94 kg·m^{-3}·K^{-1}	29.90 kg·m^{-3}·K^{-1}	32.90 kg·m^{-3}·K^{-1}
Deviation	+8.3%	+15.9%	+27.6%

on the temperature development. Therefore, the quench time has to be kept as short as possible.

Figure 3 presents the isentropic coefficients $(\Delta\rho/\Delta p)_S$ for the full density range for various 1g (top) and μg (bottom) experiments at different temperatures in comparison with the equation of state of Ref. 10. For reasons of clarity, only the results for $T_c + 1000$ mK and $T_c + 1$ mK are

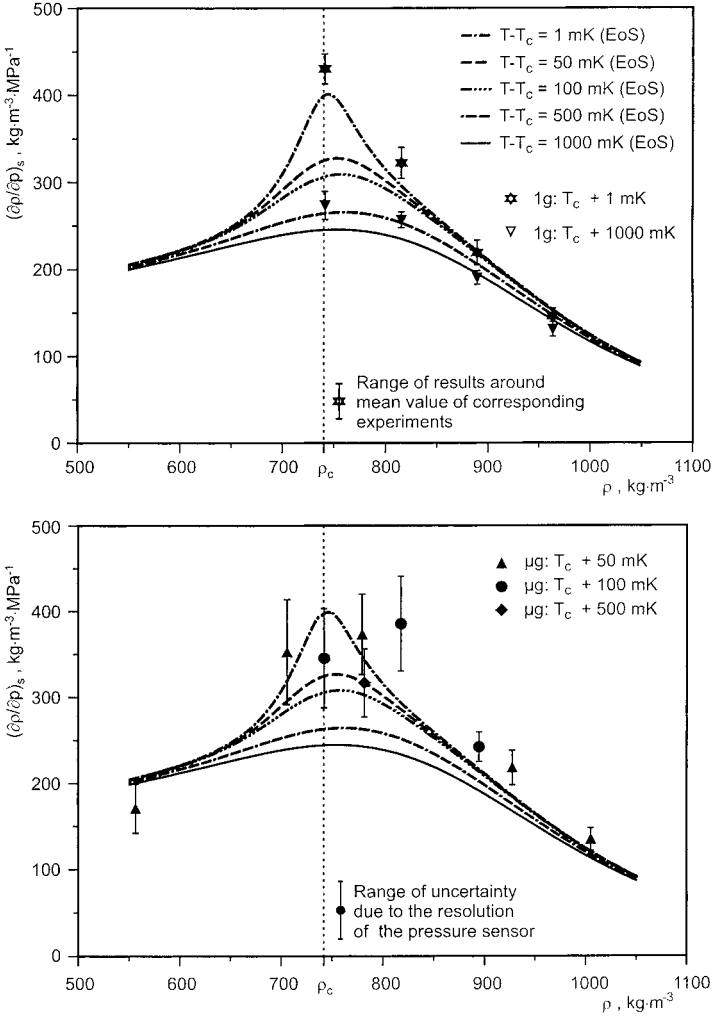

Fig. 3. Isentropic difference coefficient $(\Delta\rho/\Delta p)_S$ for various densities and temperatures under 1g (top) and μg (bottom) in comparison with the equation of state for SF_6 [10].

given; all others would be between the two extremes. As it was possible to perform far more PE experiments under 1*g*, each point represents the mean value, with the bar showing the range of values from various experiments at distinct densities. Here, the experimental results are in a reasonable range, exceeding the theoretical values by only 6 to 27%. While the deviation is smaller for far off-critical densities, it is obvious that the influence of the PE and convection is larger at critical densities, leading to a more significant deviation.

In the lower graph in Fig. 3, each coefficient results from a single μg measurement, while the error bar represents the range of uncertainty due to the resolution of the pressure sensor. In this case, the deviation from theory is also in a reasonable range, and the coefficients are again in better agreement for off-critical densities compared to the near-critical region. As the 1*g* and μg results and their deviation from theory do not differ very much from each other within the precision of our measurements, it seems that our method of rapid density quenches is less influenced by gravity, and more by the PE, which is known to be more dominant in the near-critical than in the far off-critical region [4].

In Fig. 4 our isentropic pressure coefficients are in relatively close agreement with the theoretical values from the equation of state [10] for the three densities $\rho = 1.1$, 1.2, and $1.3\rho_c$. This is true for both the 1*g* and the two μg measurements. The bar with each coefficient represents the range of uncertainty due to the resolution of the pressure sensor at the

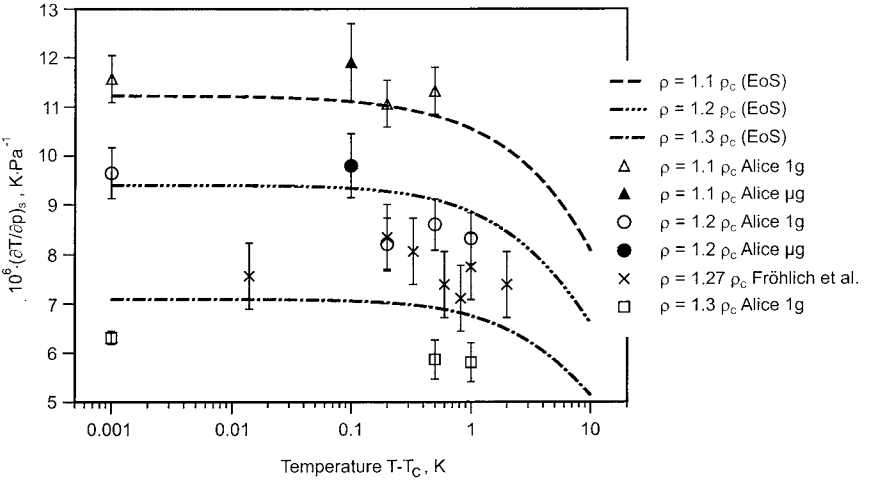

Fig. 4. Isentropic difference coefficients $(\Delta T/\Delta p)_S$ for supercritical temperatures and densities in comparison with equation of state (EoS) [10] and heat pulse experiments [5].

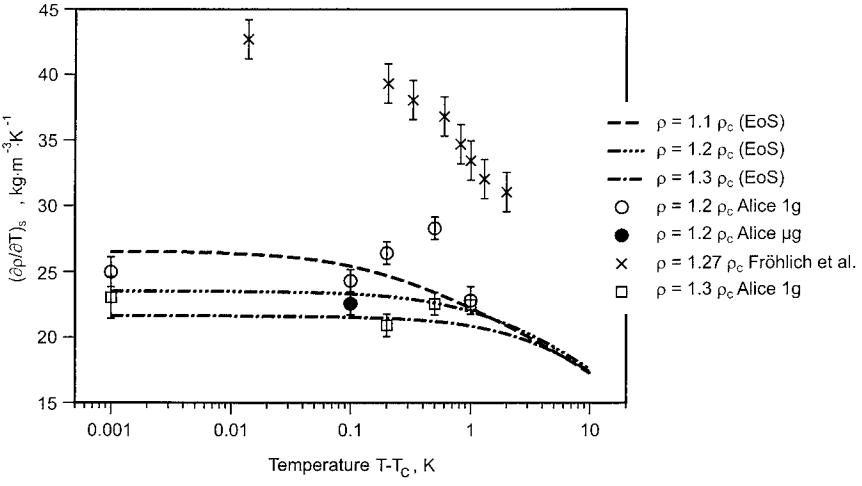

Fig. 5. Isentropic difference coefficients $(\Delta\rho/\Delta T)_S$ for supercritical temperatures and densities in comparison with equation of state (EoS) [10] and heat pulse experiments [5].

facility. In the literature one similar μg experiment [5] could be found from which isentropic coefficients were calculated. In this case temperature quenches of 15-s duration were induced into the fluid instead of density quenches. The average density in the fluid was $1.27\rho_c$; the local density change was observed by a Twyman–Green interferometer and the temporal change of the density gradient was calculated with the Lorentz–Lorenz relation. The results for the density of $1.27\rho_c$ from Ref. 5 also fit nicely within their range of uncertainty, so that both methods (temperature or density quench) qualify for the determination of the pressure coefficient.

In Fig. 5 the values of the isentropic density coefficient $(\partial\rho/\partial T)$ are presented. The bar with each point represents the uncertainty due to the temperature and density resolution. The results are also in close agreement with the equation of state [10], while Ref. 5 shows a large systematic discrepancy, in the range of 100%, for the results of the density $1.27\rho_c$.

5. CONCLUSION

It is not easy to analyze the dynamics of the PE, because thermal diffusion and conduction are not well defined near the cell walls, and due to the phenomenon's characteristic time compared to the long equilibration times of classical materials, it is difficult to realize an ideal temperature step. The fact, however, that both 1*g* and μg data are in reasonable agreement with the calculated values from the equation of state points to the

advantage of our method of measurement, which allows the calculation of the density change from mechanical settings with a sufficient accuracy. Another advantage is the rapidness of the quench, simulating step-like temperature changes in the fluid, which can be performed magnitudes faster than heat pulses to achieve the same measurable effect. This minimizes the grade of influence of convection and is therefore a good method to obtain the isentropic coefficients from ground-based experiments. The fact that the 1*g* and μg results do not seem to differ very much from each other supports the assumption that in both cases the PE dominates the temperature propagation. If convection plays a role under 1*g* conditions, its influence is so small compared to the PE that it is not recognized by the resolution of the measurement.

ACKNOWLEDGMENTS

This research was supported by Deutsches Zentrum für Luft- und Raumfahrt e.V. (DLR) under Grant 50WM9604. The above-described German μg experiments were performed on the MIR space station as part of the French MIR mission PERSEUS made possible under a French–German cooperation contract between CNES and DLR. We would like to thank B. Zappoli and J.-F. Zwilling, of the French space agency CNES, Toulouse, and Y. Garrabos and C. Chabot, of ICMCB, Bordeaux, for their support and fruitful discussions. We are also grateful to the van der Waals–Zeeman Laboratory of the University of Amsterdam for building our thermostats and are indebted to J. V. Sengers for providing us a copy of his equation of state for SF_6.

REFERENCES

1. J. Straub, L. Eicher, and A. Haupt, *Phys. Rev. E* **51**:5556 (1995).
2. A. Onuki, H. Hao, and R. A. Ferrell, *Phys. Rev. A*. **41**:2256 (1990).
3. A. Onuki and R. A. Ferrell, *Physica A* **164**:245 (1990).
4. H. Boukari, J. Shaumeyer, M. Briggs, and R. Gammon, *Phys. Rev. A* **41**:2260 (1990).
5. T. Fröhlich, P. Guenoun, M. Bonetti, F. Perrot, D. Beysens, Y. Garrabos, B. Le Neindre, and P. Bravais, *Phys. Rev. E* **54**:1544 (1996)
6. R. Marcout, J.-F. Zwilling, J. M. Laherrere, Y. Garrabos, and D. Beysens, *ALICE 2, an advanced facility for the analysis of fluids close to their critical point in microgravity*. Presented at the 45th Congress of the International Astronautical Federation, Jerusalem, Israel (1994).
7. W. Wagner, N. Kurzeja, and B. Pieperbeck, *Fluid Phase Equil.* **79**:151 (1992).
8. P. Jany, Ph.D. thesis (Technische Universität München, München, 1986).
9. Kruppa, Ph.D. Thesis (Technische Universität München, München, 1993).
10. K. Wyczalkowska and J. V. Sengers, *J. Chem. Phys.* **111**:1551 (1999).